Journal of Catalysis **187,** 298–310 (1999)
Article ID jcat.1999.2613, available online at http://www.idealibrary.com on IDEAL®

Effect of Mo on the Active Sites of VPO Catalysts upon the Selective Oxidation of *n*-Butane

S. Irusta, A. Boix, B. Pierini, C. Caspani, and J. Petunchi

Instituto de Investigaciones en Catálisis y Petroquímica, INCAPE (FIQ, UNL-CONICET), Santiago del Estero 2829, 3000-Santa Fe, Argentina

Received November 11, 1998; revised June 25, 1999; accepted June 28, 1999

The effect of the addition of Mo to VPO formulations on the physicochemical and catalytic properties of VPO solids was studied using X-ray diffraction (XRD), Fourier transform infrared spectroscopy, X-ray photoelectron spectroscopy, Laser Raman spectroscopy (LRS), temperature-programmed reduction, and a flow reactor system. The addition of Mo to the oxides increases the activity and selectivity of the VPO catalysts. The promoting effect is a function of both the Mo loading and the way such cation was added to the VPO matrix. The best catalyst was obtained when 1% Mo was impregnated on the $VOHPO_4 \cdot 0.5H_2O$ phase. At 400°C 36% of molar yield to maleic anhydride was obtained in this catalyst against 12% of the unpromoted catalysts and only 3% of the solids where Mo was added during the phosphatation step. The impregnated 1% Mo catalyst achieved a molar yield of 50% after 700 h under reaction stream (equilibrated catalysts). $(VO)_2P_2O_7$ was the only phase detected by XRD and LRS in all the catalysts studied. They showed comparable BET surface areas and crystallinity after 400 h under reaction conditions. A local order distortion of the O_3–P–O–P–O_3 structure was detected by LRS in the impregnated Mo VPO catalysts. After 400 h on stream, both promoted and unpromoted solids only showed V^{IV} on the surface layer. The main effect on the addition of Mo by impregnation to VPO oxides was enhanced by the very strong Lewis acid sites and the liability of the oxygen of $(VO)_2P_2O_7$. This suggests that the promoting effect is more electronic in nature than structural. Polymeric MO_3 species were detected neither by TPR nor by LRS. All the promoted catalysts presented a surface molybdenum enrichment but whereas the coprecipitated Mo VPO solid only shows surface Mo^{VI}, both Mo^{VI} and Mo^{IV} coexist in the impregnated catalyst. The solid with the highest yield of maleic anhydride also has the highest surface Mo^{IV}/Mo^{VI} ratio.

Key Words: **VPO catalysts; selective oxidation; *n*-butane to MA partial oxidation; promoting effect; molybdenum; LRS; XPS; FTIR.**

INTRODUCTION

VPO solids are well known as catalysts for the oxidation of *n*-butane to maleic anhydride (1). Patents deal mainly with the improvement of phosphorus–vanadium catalysts by the addition of promoters or with the use of different preparation methods of the precursor (2). While there is a considerable amount of information in the literature on the properties and characterization of solids prepared and activated by different methods, it is not possible to say the same about the effect of promoters in the VPO system (1–5). In fact, Ye *et al.* (6) studied a series of promoters on the VPO structure and on the density of the V=O sites concluding that the addition of slightly electronegative ions increased both the number of surface V=O species and the exposition of the [100] plane. On the other hand, another group of researchers (7) reported the incorporation of promoters in the $(VO)_2P_2O_7$ lattice with a uniform distribution. They found that if one of the vanadium ions is replaced by a promoter ion which has a lower electronegativity than vanadium ions, the next V^{IV} ions can withdraw more electrons from neighboring oxygen atoms so that the electron density of the V^{IV} ions is increased and then the V=O bond weakens. The specific activity increases with the decreasing vigor of the V=O bond thus suggesting that the V=O group of $(VO)_2P_2O_7$ participates in the formation of maleic anhydride. More recently, Volta and co-workers (8, 9) studied the role of Fe and Co on the activation of VPO catalysts, showing that depending upon their oxidation potential and dispersion, promoters control the V^V/V^{IV} ratio during the activation period, thus affecting the behavior of the catalysts obtained. Several authors (5, 10, 11) have already remarked on the importance of the redox couple between V^{IV} and V^V on the reaction mechanism.

In the literature of patents, Mo frequently appears as promoter. Hutchings (2, 12) reported that the optimal amount of aggregated Mo is V : Mo = 1 : 0.04, increasing the specific activity of the catalyst and the yield to maleic anhydride. Ye *et al.* (6) found that Mo increases reaction rate and selectivity to MA. They claimed that the promoter changes the exposure of the [100] plane and the disorder along this plane, suggesting that the activity of individual sites increase with this disorder. In the same vein, Bej and Rao (13) reported that Mo and Ce simultaneously added to VPO oxides produced higher yield of maleic anhydride as compared to the unpromoted oxides. They suggested that such a behavior may be due to the fact that molybdenum prevents further reduction of V^{IV} to V^{III}, whose transformation was probably responsible for the production of

0021-9517/99 $30.00

carbon oxides. However, Takita *et al.* (7) adding Mo by a novel preparation method found that the MA yield is lower than for VPO. They reported that the promoter ions are uniformly dispersed into the $(VO)_2P_2O_7$ crystal lattices. Despite all these publications, the promotion effect of Mo has not yet been well elucidated. This work makes a comparative study of VPO catalysts containing different quantities of Mo, added by impregnation or coprecipitation. The solids were characterized through X-ray photoelectron spectroscopy (XPS), temperature-programmed reduction (TPR), Fourier transform infrared spectroscopy (FTIR), and Raman spectroscopy trying to find the Mo role over the active sites for the *n*-butane partial oxidation to maleic anhydride.

EXPERIMENTAL

Catalysts preparation. In order to obtain the precursor phase, V_2O_5 was refluxed in a reducing mixture of bencylic and *i*-butylic alcohol for 3 h; afterward, the necessary amount of phosphoric acid (100%) to obtain a P/V ratio of 1.28 was added, keeping it in reflux during 2 h. The solid thus obtained was filtrated and dried in a stove at 150°C for 24 h. The molybdenum-containing precursor phases were obtained by two different ways.

1. Coprecipitation: the necessary amount of ammonium heptamolybdate to obtain 1 and 5% (w/w) of Mo was added together with the phosphoric acid, following the same procedure applied for VPO.
2. Incipient wetness impregnation: the obtained precursor, already dried in a stove, was impregnated with an ammonium heptamolybdate solution and later dried again. By this latter method solids with 1, 3, and 5% (w/w) of molybdenum were prepared.

Table 1 shows characterization data of the solids prepared. It was estimated that with 1% (w/w) of Mo, only 20% of the surface would be covered, while with 5% (w/w) of Mo a monolayer could be formed. Pure phases of V^{IV} and V^{V} $(VO)_2P_2O_7$, α_1VOPO_4, β-$VOPO_4$ were prepared by starting from organic (V^{IV} phase) and aqueous precursor (V^{V} phase), respectively. Pure $(VO)_2P_2O_7$ was obtained by calcining the precursor in N_2 at 750°C for 120 h whereas the V^{V} phase was calcined in air at 650°C for 120 h. Further details of preparation and characterization of the pure phases have been given elsewhere (14, 15).

TABLE 1

Preparation Techniques and Content of VPO Solids

Catalyst[a]	Mo loading (% w/w)[b]	Mo/V[c] (atomic ratio)	Way of adding Mo
VPO	—	—	—
VPOMo1	1	0.02	Impregnation
VPOMo3	3	0.06	Impregnation
VPOMo5	5	0.10	Impregnation
VPOMo1(co)	1	0.02	Coprecipitation
VPOMo5(co)	5	0.10	Coprecipitation
VPO + Mo5	5	0.10	Mechanical mixture

[a] Bulk P/V ratio, 1.28.
[b] From chemical analysis.
[c] $Mo/(VO)HPO_4 \cdot 0.5H_2O$.

A mechanical mixture of VPO and heptamolybdate was prepared so as to obtain 5% (w/w) of Mo. This mixture was calcined at 400°C. Mechanical mixtures of pure phases of V^{IV} and V^{V} (α_1VOPO_4, β-$VOPO_4$) were also prepared.

Catalytic evaluation. The catalytic evaluation was carried out in a continuous-flow reactor. *n*-Butane (0.8%) in air was fed; two space velocities were used, GHSV = 900 and 2500 h^{-1}; and the temperature range was between 320 and 440°C. The analysis of reactants and products was chromatographically performed with an AT-1200 column and a FID detector.

Activation. The precursors activation was performed *in situ* before the catalytic test. A mixture of 0.8% of *n*-butane in air was fed, with a flow of 20 ml/min. It was heated from room temperature up to 280°C at a rate of 3°C/min; it was left at this temperature for 1 h and afterward it was heated again up to 380°C at the same rate, leaving it at this temperature for 3 h.

The VPOMo1 solid was also subjected to a slow activation procedure to obtain an equilibrated catalyst in the following way:

The precursor was heated in a mixture of *n*-butane and air (0.6% *n*-butane) from room temperature to 280°C at 3°C/min. It was kept at 280°C for 16 h; then, it was heated up to 380°C and the temperature was not changed for 3 h using GHSV = 900 h^{-1}. Afterward, the temperature was increased to obtain a conversion of about 80%. This occurred very slowly, increasing the composition to 0.8% *n*-butane in air and GHSV to 2500 h^{-1}, varying the temperature between 300 and 440°C.

The equilibrated catalysts are those which did not show any changes in the catalytic performance at GHSV = 2500 h^{-1} and 0.8% *n*-butane concentration for at least 50 h after finishing the activation period (more than 650 h under reaction stream in this study).

Surface area and XRD. For the determination of the specific surface of precursors and used catalysts, a Quantachrome Sorptometer, Nova 1000 model was employed. Prior to their BET analysis all the samples were maintained at 105°C for 12 h in a stove, keeping them at 340°C under vacuum of 10^{-5} Torr for 3 h.

The X-ray diffraction (XRD) spectra of precursors and catalysts were obtained with a Shimadzu diffractometer

XD-D1 Model, using Cu K_α radiation at 30 kV and 30 mA. The scan rate was 1° min^{-1} for values between 10 and 40°.

FTIR. In order to obtain the absorption bands from the used catalysts, a Shimadzu 8101 spectrometer was used. The powder from the used catalysts was compressed at 9 ton/cm^2 in order to obtain self-supported pellets of 1 cm diameter. They were placed on a transportable cell with KBr windows.

Vacuum equipment was used for the pretreatment and the heating was performed with an external oven. The pretreatment consisted in degassing at 450°C for 12 h, in a 10^{-5} Torr vacuum. After cooling up to room temperature, the pellet spectrum was taken. The same pretreatment was performed before 35 Torr of acetonitrile were adsorbed and left in contact for 10 min.

Spectra were taken with acetonitrile in the gas phase and after evacuation of the cell at room temperature, 80 and 150°C, respectively.

Table 2 shows the IR band assignment of the V=O, P–O vibration of different VPO phases and acetonitrile adsorption bands in such oxides.

Laser Raman spectroscopy (LRS). The Raman spectra were obtained with a Jasco Spectrometer Model TRS-600-SZ-P. The excitation wavelength used was 514.5 nm from Ar^+ ion laser and the laser power, 40 mW. The LRS experiments were made at a low wave number (400–1200 cm^{-1}). The samples studied at room temperature were the solids after the catalytic test (*ex situ*). The acquisition time was 120 s. The spectra obtained under those conditions were not modified. Consequently, the samples were not altered by the laser beam.

TABLE 2

Wave Numbers and Vibration Assignment in β-$VOPO_4$, $(VO)_2P_2O_7$, α_1-$VOPO_4$, and Acetonitrile Adsorbed on VPO

Solid	Band position (cm^{-1})	Assignment	Reference
β-$VOPO_4$	995	νV=O	20
	998	νV=O	21
	987	P–O–V	21
	940	ν_sP–O	20
$(VO)_2P_2O_7$	1002	νV=O	22
	966	νV=O	19
	935	ν_{as}P–O–P	21
	920		
α_1-$VOPO_4$	991	νV=O	22
	926	ν_{as}P–O–P	—
	Acetonitrile-adsorbed bands and assignment		
VPO	2252	νCN (H-bonded acetonitrile)	17
	2275	Medium strong Lewis acid sites	17
	2207	Fermi resonance of νCN with $\nu_3+\nu_4$	17
	2328	Very strong Lewis acid sites	17

XPS. The spectra were obtained with a Shimadzu Esca 750 spectrometer using nonmonochromatic radiation Mg K_α at room temperature. The data collected using an ESCA PACK 780 computer interface to the spectrometer were analyzed with a Goodgly software developed at the University of Pittsburgh. The binding energies were referred to the C1*s* signal (284.6 eV). The curves were fitted with Gaussian–Lorentzian functions. The O1*s* satellite peaks overlapped with the V2$p_{1/2}$ signal; consequently the V2$p_{3/2}$ signal was used. The spin–orbit separation of 7.2 eV and the V2$p_{1/2}$/V2$p_{3/2}$ = 0.5 intensity ratio were additional considerations for the adjustment of the V2*p* doublets. For Mo3*d*, the Mo3$d_{5/2}$/Mo3$d_{3/2}$ = 1.5 ratio and the spin–orbit separation of about 3.3 eV were also considered.

The atomic ratios $(O/V)_s$, $(P/V)_s$, and $(Mo/V)_s$ were calculated using the areas under the O1*s*, P, and V2$p_{3/2}$ peaks, the Scofield photoionization cross-sections, the mean free paths of the electrons, and the function given by the instrument.

TPR. The temperature-programmed reduction experiments were performed in a flow instrument with a thermal conductivity detector (TCD). One-hundred milligrams of solid was used and the reducing gas was a 5% H_2/Ar stream (with a heating rate of 10°C/min from room temperature up to 750°C).

RESULTS

Catalytic measurements. The catalytic behavior at GHSV = 900 h^{-1} and 0.8% *n*-butane in air of nonequilibrated VPO, VPOMo1(co), and VPOMo5(co) and VPOMo1 (solid with impregnated molybdenum) is shown in Fig. 1.

The two catalysts with 1% of molybdenum have a similar activity (Fig. 1A) independent of the way in which Mo was incorporated. In both of them, the conversion of *n*-butane was higher than for the solid without promoter. Instead, the activity of VPOMo5(co) was slightly lower than that of VPO. However, the Mo added by coprecipitation decreases the selectivity to maleic anhydride (Fig. 1B) this drop being even more stressed for the solid with a lesser charge, VPOMo1(co), whereas when the promoter is added by impregnation, the selectivity to MAN is higher than in the unpromoted catalyst, even at high conversions. In view of these results, the effect of Mo loading (added by impregnation) on the activity and selectivity was explored. Results obtained with 1, 3, and 5% Mo compared with VPO at three different temperatures (340, 360, and 380°C) are reported in Figs. 2A and 2B. It can be observed that the catalyst with the lowest content of Mo produces the best conversion and yield to maleic anhydride, both decreasing for higher loading of the promoter in the whole range of temperatures (320–420°C). When all the solids were studied at high space velocity (GHSV = 2500 h^{-1}) no changes were observed in

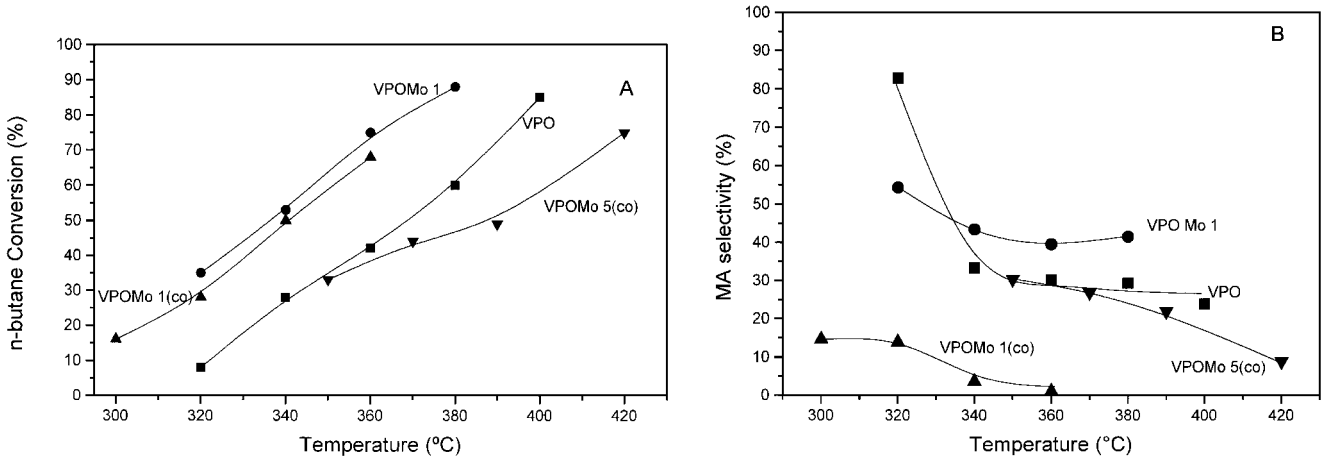

FIG. 1. Effect of the reaction temperature on *n*-butane conversion (A) and percentage of selectivity to maleic anhydride (B). Reaction conditions: 0.8% C_4H_{10} in air; GHSV = 900 h^{-1}.

their behavior. The same trend was found in equilibrated catalysts but now a 50% yield to maleic anhydride was obtained at 400°C in VPOMo1. In order to corroborate this trend, the MAN yield was plotted as a function of temperature for the equilibrated and nonequilibrated solid with 1% Mo (VPOMo1) (Fig. 3).

Taking into account the above catalytic behavior of Mo-containing VPO samples, a systematic volumetric and surface characterization of the solids was done in order to ascertain the effect of Mo in the properties of VPO and how they correlate with the catalytic behavior of such compounds.

XRD. The XRD patterns of undoped and doped precursors only show the characteristic lines of $VOHPO_4 \cdot 0.5H_2O$. The nonequilibrated and equilibrated catalysts with and without Mo present the XRD patterns characteristic of $(VO)_2P_2O_7$. In no case were V^V or $MoOPO_4$ detected. In order to obtain additional information on the effect of the promoter on the morphology of the catalysts crystallite, the method described by Contractor and co-workers (16) was employed which enabled us to determine the thickness and length of the [100] plane of the $(VO)_2P_2O_7$ which are shown in Table 3.

It can be noticed that the impregnation method does not greatly alter the thickness of the [100] or [042] plates. Besides, all materials present similar areas which correlate with the thickness and with the platelet shape of the pyrophosphate. The R_c ratio of the promoted catalysts is lower than those of the VPO catalyst ($R_c = 2.6$) but they show a comparable crystallinity degree to VPO solids.

The promoted catalysts prepared by coprecipitation also present comparable surface area despite the different thickness of the crystallite and R_c value (Table 3).

Regarding the degree of disorder of plane [100], the last column of Table 3 includes the information concerning the linewidth of this plane. It can be observed that solids impregnated with molybdenum present a broadening similar

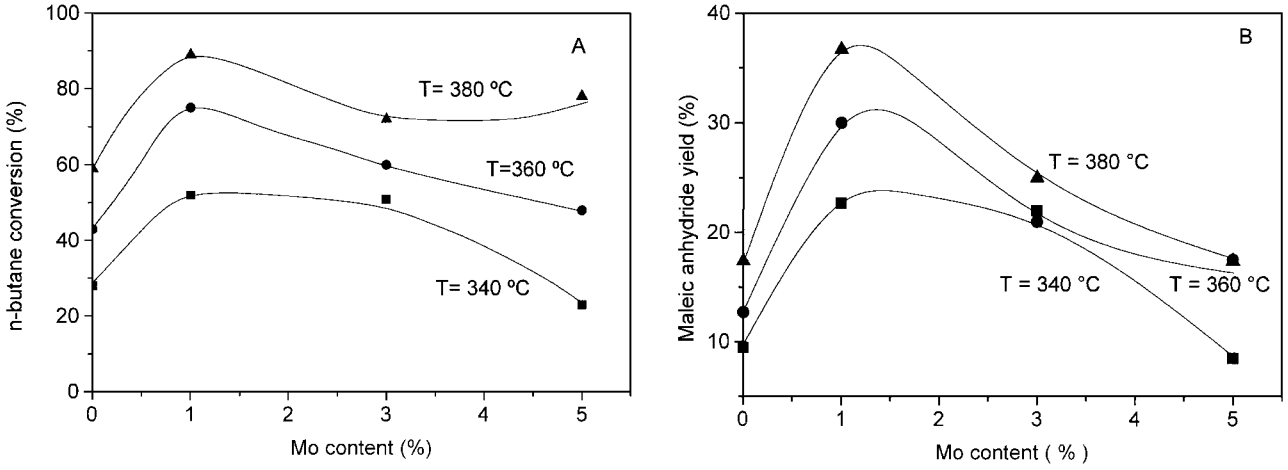

FIG. 2. Effect of Mo content on *n*-butane conversion (A) and maleic anhydride yield (B) at different temperatures. Reaction conditions: see Fig. 1.

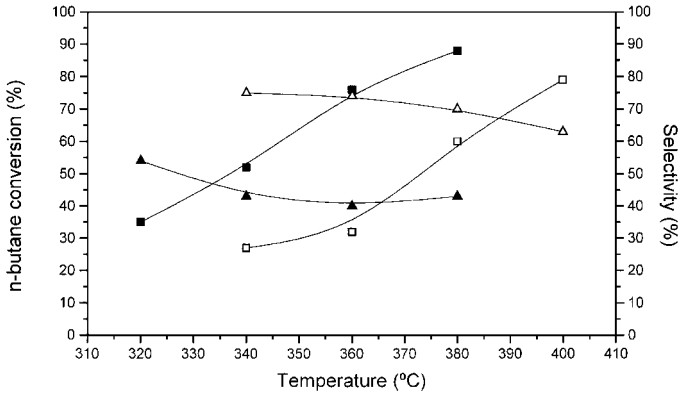

FIG. 3. Catalytic behavior of equilibrated (open symbols) and nonequilibrated (solid symbols) VPOMo1. (squares) Conversion; (triangles) selectivity. Reaction conditions: see Fig. 1.

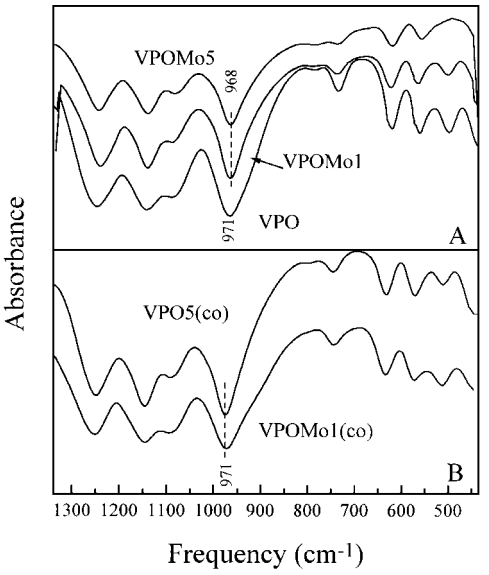

FIG. 4. Effect of Mo on the structural FTIR spectra of VPO. (A) Supported MoVPO catalyst. (B) Coprecipitated MoVPO catalyst.

to that of VPO, which was in agreement with the linewidth presented by an equilibrated catalyst. It should be remarked that the greatest degree of disorder appears in the case of samples with 1% Mo obtained by coprecipitation.

FTIR. This technique was employed to analyze the influence of Mo on the V=O species in the matrix of $(VO)_2P_2O_7$ and the effect of the addition of such cation in the acid sites of the VPO catalysts. Figure 4 presents the infrared spectra obtained for the VPO catalyst and for the VPO catalyst with Mo added by impregnation (Fig. 4A) and coprecipitation (Fig. 4B). VPO and VPOMo show typical $(VO)_2P_2O_7$ bands (Table 2) but a certain distortion in the PO_4 region (1100 to 1300 cm^{-1}) is noticeable (compare Figs. 4 and 5A).

Focusing attention on the band corresponding to V=O, it is possible to observe that while in the pure pyrophosphate phase, in VPOMo1(co) and in VPOMo5(co) this band appears at 971 cm^{-1} (Figs. 4B and 5A), in the other solids (VPO and VPO with impregnated Mo) it shifted to 968 cm^{-1}. Besides, a broadening to the low frequency zone is observed (Fig. 4A). In no case was the V=O stretching band of V^V (Fig. 5A and Table 2) observed.

The broadening of the band in the 900–1100 cm^{-1} region (Fig. 4A) could be related with the ν_sP–O band (947 cm^{-1}) which appeared in the α and β phase (Fig. 5A). In order to verify this possibility a mechanical mixture of α-$VOPO_4$ (V^V) and $(VO)_2P_2O_7$ (V^{IV}) pure phase were prepared to obtain 80, 60, 40, and 20% (w/w) of V^{IV}. FTIR spectra of these mixtures are shown in Fig. 5B. It can be observed that as the proportion of V^V increases, the signal appearing at 971 cm^{-1} for the pure V^{IV} phase ($(VO)_2P_2O_7$) (Fig. 4A) broadens and the maximum lightly shifting to lower frequencies. The separation between the bands at 995 cm^{-1} (V=O) and 947 cm^{-1} (ν_sP–O), characteristic of V^V, was

TABLE 3

Mo Effect on the Crystallite Structure of VPO Solids

Catalyst	BET area (m^2/g)	Degree of crystallinity (%)[a]	Thickness[b] [042]	Thickness[b] [100]	R_C[c]	Linewidth[d] (°) [100]
VPO	19.5	63	202.64	72.87	2.6	1.1
VPOMo1	22.0	58	202.60	80.14	2.5	1.0
VPOMo3	22.7	68	162.07	80.15	2.0	1.0
VPOMo5	21.0	65	147.37	89.07	1.6	0.9
VPOMo1co	22.7	62	202.67	57.27	3.5	1.4
VPOMo5co	21.0	63	147.37	106.00	0.8	0.6

[a] Degree of crystallinity, $1/[1 + k(I_A/I_C)]$. I_A and I_C are the intensity of X-ray patterns from the amorphous and the crystalline portions of the samples, respectively, and K is the crystalline/amorphous relative response factor.
[b] Plate thickness (Å) by means of Scherrer's formula: $T(Å) = 0.89 \cdot \lambda/\text{FWHM} \cdot \cos\theta$.
[c] R_C, ratio of FWHM of [100]/[042] XRD lines, $2\theta = 22.8°0$ and $2\theta = 28.5°$, respectively.
[d] FWHM of [100] lines.

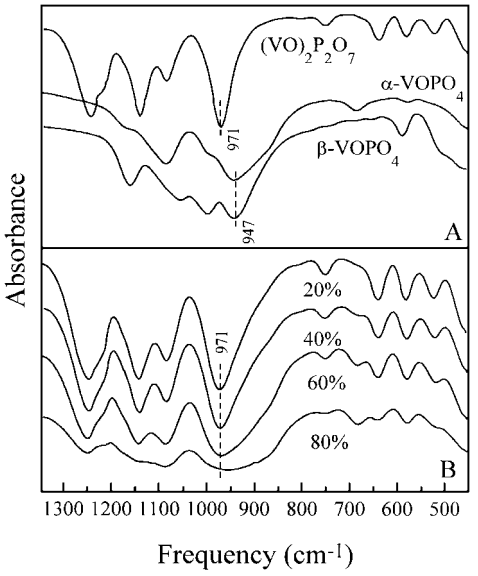

FIG. 5. Structural FTIR spectra of (A) pure VPO phases: $(VO)_2P_2O_7$, $\alpha VOPO_4$, and $\beta VOPO_4$. (B) Mechanical mixture of $(VO)_2P_2O_7$ and $\alpha VOPO_4$ phase calcinated at 400°C. 20, 40, 60, and 80% of V^{IV}, respectively.

not observed in the mechanical mixtures. The above results clearly show that the presence of V^V phase increases the band width of the V=O stretching. This could suggest that in both VPO and VPOMo catalysts some V^V are present.

Acetonitrile adsorption. Cornaglia *et al.* (17) and Busca *et al.* (18) have reported that acetonitrile, a base weaker than NH_4 or pyridine, is a more sensitive molecule probe to differentiate between Lewis acid sites of varying strengths. Therefore, in attempting to determine the effect of Mo in such acid sites in VPO oxides acetonitrile was adsorbed on unpromoted catalysts (VPO) and Mo-containing VPO adding either by impregnation (VPOMo1) or coprecipitation (VPOMo1(co) (Figs. 6A and 6B)). In further agreement, the species responsible for the maximum at 2253 cm^{-1} (which is assigned to the hydrogen-bonded acetonitrile (17, 18) was progressively removed after treatment at 150°C. (Fig. 6B). Noticeably, a band at 2265 cm^{-1} was detected in VPO and VPOMo1 samples after such treatment, but that band was not observed in the VPOMo1(co) sample (Fig. 6B). This band could be related to the one reported by Busca *et al.* (18) at 2275 cm^{-1} and by Cornaglia *et al.* (17) at 2280 cm^{-1} and attributed to medium-strong Lewis sites. The two strong bands of similar intensities at 2300 and 2326 cm^{-1} were the ones that remained. The bands at 2295 and 2328 were assigned to the adsorption of acetonitrile at very strong Lewis acid sites (17, 18), the first one due to the Fermi resonance of νCN with $\nu_3 + \nu_4$. From what is said above, it could be suggested that in the Mo-promoted catalyst prepared by coprecipitation a lower concentration of such acid sites could exist.

XPS. Table 4 shows the XPS data of the pure compounds and catalysts after having been used in the catalytic evaluation. The data of the pure compounds are used to identify the possible changes occurring on the surface of the catalysts after being in contact with the reactant stream. $(VO)_2P_2O_7$ exhibits two peaks at 525.0 and 517.8 eV due to $V^{IV}2p_{1/2}$ and $V^{IV}2p_{3/2}$, respectively. In the case of the β-$VOPO_4$ (V^V) phase, the signal appears at higher binding energies, 525.5 ($V^V2p_{1/2}$) and 518.8 eV ($V^V2p_{3/2}$) in agreement with what was reported by Cornaglia and Lombardo (14).

In Table 4 (fifth column) the difference in BEs of O1*s*-$V^{IV}2p_{3/2}$ is also shown. This parameter is used to determine the oxidation state of vanadium on the surface of vanadyl phosphate and other solids containing mixtures of the VPO phase. Notice that the pure V^{IV} phase $(VO)_2P_2O_7$ shows a ΔO1*s*-V2*p* = 14.4 while the pure V^V phase β-$VOPO_4$ shows a ΔO1-V2p = 12.9. The Δ values for the used unpromoted catalyst is slightly smaller than those found for the pure phase (viz $\Delta_{O1s\text{-}V2p} = 14.3$).

The addition of promoters either by impregnation or by coprecipitation modifies neither the binding energy value nor the FWHM with respect to the unpromoted catalyst. Besides, the Δ values for the impregnated promoted catalyst do not differ from those of the VPO catalyst. However, in the solid with Mo added by coprecipitation, those values depend on the Mo loading. Solids with 1% Mo the Δ value is the same as in the pure $(VO)_2P_2$ phase, while the samples with 5% Mo have a lower Δ value.

The BEs of the P2*p* and O1*s* are the same in all the catalysts studied. They are the same values as in the pure

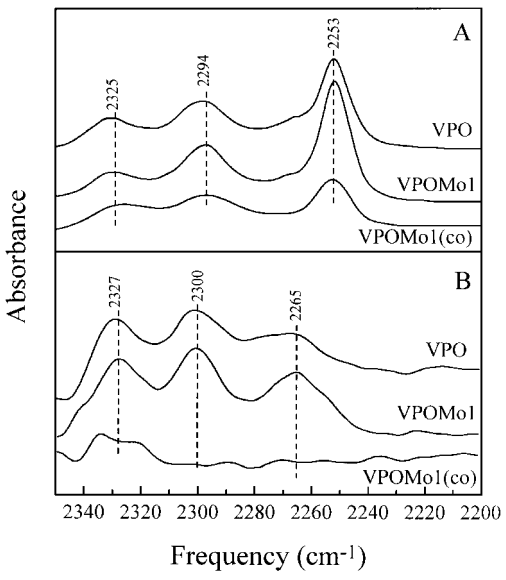

FIG. 6. FTIR spectra of acetonitrile adsorbed at room temperature and after evacuation at room temperature (A) and 150°C (B): unpromoted VPO catalyst, VPOMo1, and VPOMo1(co). In all cases before the FTIR experiments, catalysts were under reaction conditions for 400 h.

TABLE 4

XPS Data of Pure Phases and Catalysts

Catalysts	Binding energy, FWHM (eV)[a]				Surface ratio[c]	
	O1*s*	P2*p*	V2$p_{3/2}$	$\Delta_{O\,1s\text{-}V2p}$[b]	O/V	P/V
Phases						
β-$VOPO_4$	531.1 (2.0)	133.6 (2.0)	518.2 (2.0)	12.9	5.1	1.2
$(VO)_2P_2O_7$	532.3 (2.7)	134.0 (2.1)	517.8 (2.3)	14.4	4.8	1.2
Catalysts						
VPO	532.3 (2.5)	134.3 (2.1)	518.0 (2.1)	14.3	7.8	2.6
VPOMo1	532.3 (2.9)	134.3 (2.2)	518.0 (2.3)	14.3	9.5	2.9
VPOMo5	532.2 (2.4)	133.9 (2.1)	517.9 (2.3)	14.3	7.1	2.5
Catalysts						
VPOMo1(co)	532.2 (2.5)	134.0 (2.2)	517.8 (2.5)	14.4	9.0	2.3
VPOMo5(co)	532.0 (2.0)	134.0 (2.2)	517.8 (2.2)	14.2	9.9	2.1

[a] Referenced to BE of C1*s* 284.6 eV; numbers between brackets are the full widths at half maximum, in electron volts (eV).
[b] Difference in binding energies between O1*s* and V2$p_{3/2}$ (eV).
[c] Surface ratio calculated from XPS data (see Experimental).

$(VO)_2O_2P_7$ phase. However, the surface O/V and P/V ratios were higher than the O/V stoichiometric ratio of $(VO)_2P_2O_7$ and the bulk P/V ratio (4.5 and 1.25, respectively, in agreement with Cornaglia *et al.* (19) (Table 4). XPS data also show the surface of molybdenum enrichment (compare Table 1 and Table 5). Interestingly, in the impregnated promoted catalyst some Mo^{IV} is observed on the surface (BE 231.8, FWHM 2.1) while in the coprecipitation promoted catalysts, only Mo^{VI} is observed (BE 232.6, FWHM 2.7) (Table 5).

LRS. In this study we intend to determine the presence of V^{IV} and V^{V} phases and how they can by affected by the presence of Mo.

The 400–1200 cm^{-1} range was employed. In this range intense, acute bands can appear corresponding to: (i) the stretching of M=O species (V=O, Mo=O) in the region close to 1000 cm^{-1}, (ii) symmetric and asymmetric P–O–P stretching band at 915 and 730 cm^{-1}, (iii) weak bands in the bending region at ~500 cm^{-1}, and (iv) V–O–P stretch ca. 1000–1100 cm^{-1}.

TABLE 5

XPS Data of Mo3*d*

Catalyst	Binding energy Mo3$d_{5/2}$[a]		Surface ratio[b]	
	Mo^{VI}	Mo^{IV}	Mo^{IV}/Mo	Mo/V
VPOMo1	233.0 (2.4)	231.8 (2.1)	0.22	0.2
VPOMo5	232.5 (2.7)	231.5 (2.1)	0.13	0.3
VPOMo1(co)	232.6 (2.7)	—	—	0.1
VPOMo5(co)	232.8 (2.6)	—	—	0.4

[a] Reference BE of C1s 284.6 eV; numbers between brackets are the full width at half maximum.
[b] Surface ratio calculated from XPS data (see Experimental).

Figure 7 shows the well-crystallized pyrophosphate and the MoO_3 spectra taken as reference. Two catalysts of 1% Mo are also included (impregnated and coprecipitated) as well as an unpromoted VPO solid. The well-crystallized vanadyl pyrophosphate presents very intense bands at 924 and 920 cm^{-1}. As a matter of fact, both appear as a sole band which is split in two peaks at the maximum; additional bands appear at 1185 and 1130 cm^{-1}. It is a very clear spectrum where the less intense signals are almost imperceptible compared with the band at 920–924 cm^{-1}.

The phosphorus atoms linked to a central O (O_3P–O–PO_3) are structures which, if assumed planar (P–O–P), form a binding angle of 115° and present signals active to Raman at 915 cm^{-1} (ν_{as}) and 730 cm^{-1} (ν_s) (20). The results in Fig. 7 suggest that the angle is bigger and, accordingly, the signal is shifted to higher frequencies thus denoting the presence of some distortion in the well-crystallized $(VO)_2P_2O_7$ phase. On the other hand, there are the contributions of the three P–O bindings of the PO_3 structures (signal at 1185 cm^{-1}).

Still about Fig. 7, in the spectra corresponding to MoO_3, the Mo=O characteristic band at 990 cm^{-1} is present, which is related to the symmetric stretching of mono-oxo terminal bindings. The other bands at 809 and 657 cm^{-1} correspond to Mo–O–Mo or O–Mo–O stretchings according to (21). The band at 809 cm^{-1} corresponds to a structure where Mo would have a tetrahedral coordination (22) while the one at 657 cm^{-1} would correspond to an octahedral coordination structure. These bands would eventually appear at higher Mo loadings since if MoO_3 particles existed, it is possible that they would appear highly dispersed and isolated not being able to form Mo–O–Mo polymeric associations.

In the analyzed cases, 1, 3 and 5% of Mo over VPO, the most intense expected band is the 990 one which under hydration conditions may be shifted due to the presence of

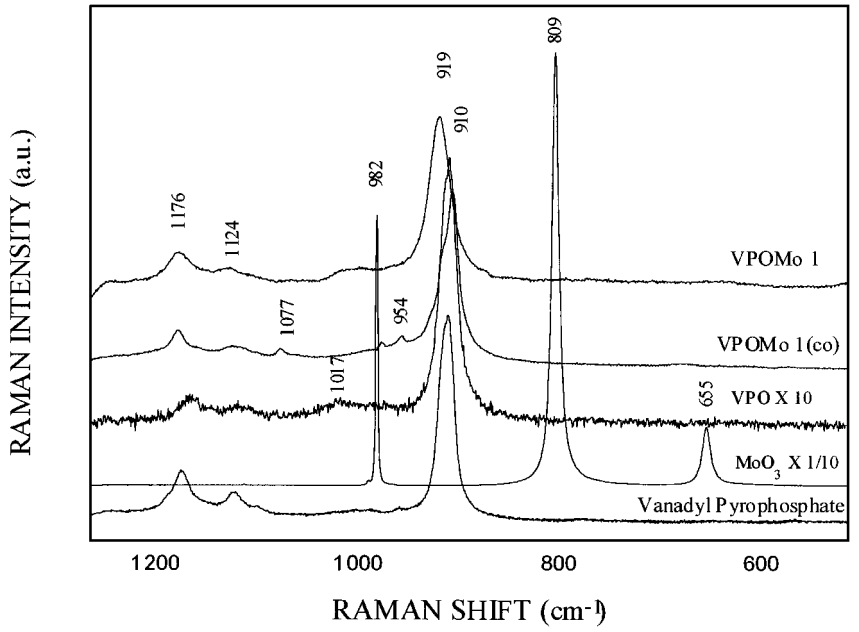

FIG. 7. Raman spectra of promoted (impregnated and coprecipitated) and unpromoted VPO catalysts, compared with pure $(VO)_2P_2O_7$ and MoO_3 phases. Before the Raman experiment, catalysts were under reaction conditions for 400 h.

coordinated protons of the Mo–O binding support oxygen atoms.

For all the promoted solids under analysis (impregnated and coprecipitated) there appears a very intense, main band in the 920–930 cm^{-1} region, with a more or less important broadening. This signal has been assigned to ν_a[P–O–P] of $P_2O_7^{-4}$ in the $(VO)_2P_2O_7$ structure.

From the comparison, it can be seen that the coprecipitated 1% Mo catalyst shows a better definition of the bands, presenting a maximum at 920 cm^{-1}—the same as the unpromoted catalyst—whereas VPOMo1 presents a broadening of such band with a shift to 933 cm^{-1}. This was not affected by the Mo loading (Fig. 8). The signals appearing in the coprecipitated 1% Mo catalysts are repeated in the catalyst

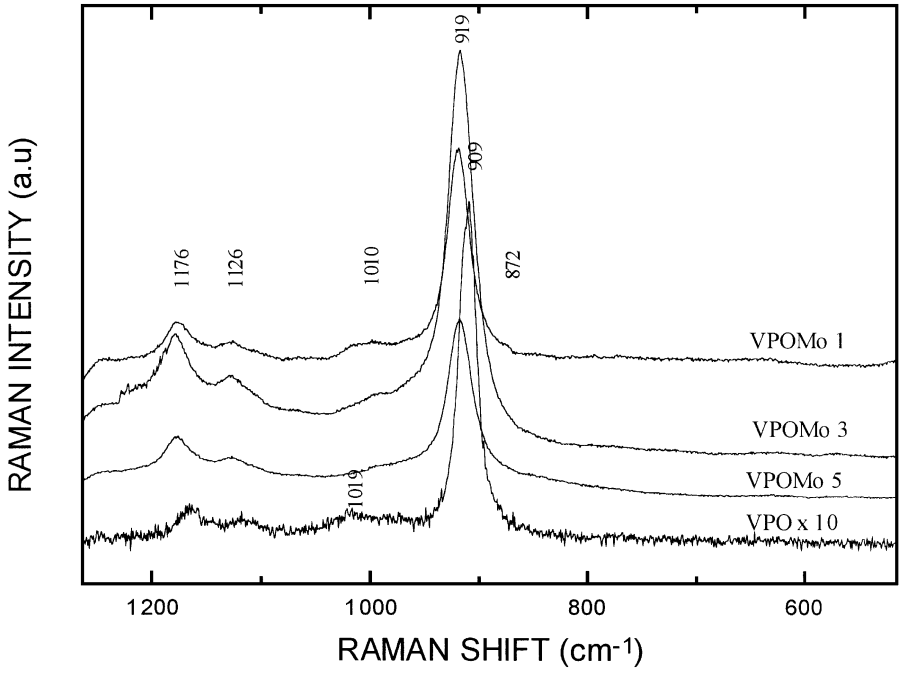

FIG. 8. Effect of the Mo loading in the Raman spectra of VPO catalysts (see Fig. 7).

TABLE 6

Raman Bands Assignment of V–O in $(VO)_2P_2O_7$

Binding	R (Å)[b] (binding length)	ν (cm^{-1})
$V–O_1$	2.15	302
$V–O_2$	1.91	547
$V–O_3$	1.60	992
$V–O_4$	2.26	243

[a] The pyrophosphate structure may be schematically represented as follows:

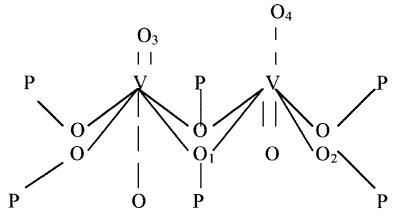

[b] R, V–O binding length.

with 5% Mo (spectrum not shown). The MoO_3 bands corresponding to Mo–O–Mo bindings appear in neither case.

A higher degree of interaction or a greater effect is expected due to the addition of Mo during phosphatation but up to a 5% loading it cannot be seen that Mo provokes changes in the pyrophosphate structure, except to accelerate the development of the present phase.

TPR. Table 7 shows the temperature-programmed reduction results of the used catalysts. With comparative purposes, the TPR of a mechanical mixture of the VPO catalyst with ammonium heptamolybdate prepared to obtain 5% (w/w) of Mo, calcined at 400°C, was included. In order to estimate the mole H_2/mole V ratio in the Mo-promoted VPO samples, the following procedure was used. From the total H_2 obtained from the integrated area of TPR profile, the hydrogen consumed to reduce Mo was subtracted. This was obtained from the mechanical mixture assuming:

TABLE 7

Effect of Mo in the Reducibility of Vanadium on VPO Catalysts

Catalyst	Mol V[a] $\times 10^4$	Mol Mo[a] $\times 10^4$	Moles of H_2 cons.[b] $\times 10^4$	$H_2/(V+Mo)$	H_2/V[c]
VPO	6.50	—	2.77	0.42	0.42
VPOMo1	6.43	0.105	3.50	0.54	0.50
VPOMo3	6.30	0.315	3.75	0.57	0.47
VPOMo5	6.17	0.525	4.18	0.62	0.46
VPOMo1co	6.43	0.105	2.46	0.37	0.34
VPOMo5co	6.17	0.525	3.33	0.50	0.32
VPOMoMM	6.17	0.525	4.0	0.60	0.42

[a] Containing 100 mg of catalyst.
[b] From TPR data.
[c] See Experimental.

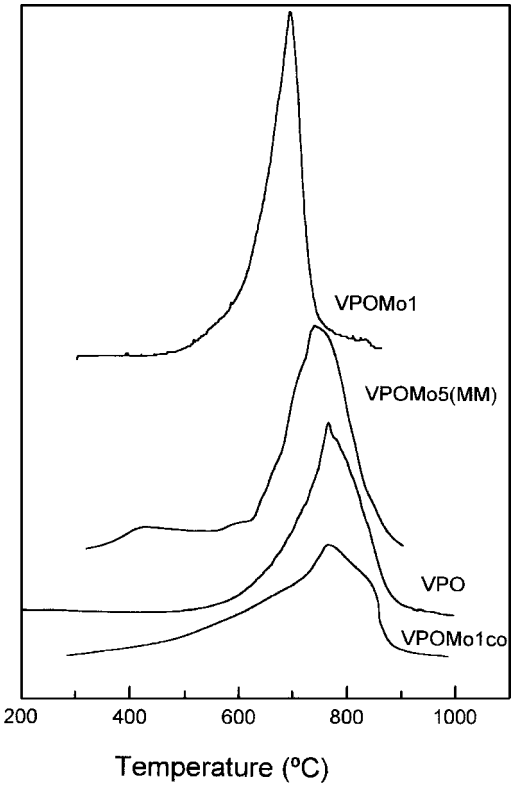

FIG. 9. Effect of the preparation method in the TPR profile of promoted VPO catalysts (VPO), unpromoted catalysts (VPOMo5MM), mechanical mixture of VPO catalysts after being under reaction for 400 h, and ammonium heptamolybdate (see Experimental). (VPOMo1) impregnated 1% Mo VPO catalysts. (VPOMo1Co) coprecipitated 1% Mo VPO catalysts.

(i) The reduction of vanadium in VPO oxides was not affected by the presence of Mo (viz. mol H_2/mol V = 0.42)

(ii) The extent of reduction of Mo in the mechanical mixture was the same as in the VPOMo and VPOMo (co) samples (viz. mol H_2/mol Mo = 1.23).

Figure 9 shows the TPR profile of some of the samples studied. VPO solids and the one with 1% of Mo added by coprecipitation presented a maximum around 750°C. Interestingly, in the Mo-impregnated VPO the maximum shifted to lower temperature (viz. 700) and the hydrogen consumed per mole of vanadium was the higher of all the solids studied (viz. $H_2/V = 0.5$).

DISCUSSION

The results obtained in this work clearly show that the addition of Mo to VPO oxides increases yields to maleic anhydride (Fig. 2) and specific activity of such solids (Table 8). This promoting effect is a function of both the Mo loading and the way in which such cation was added to the VPO matrix (Figs. 1 and 2).

TABLE 8

Initial Rate of *n*-Butane Partial Oxidation and Maleic Anhydride Production

Catalyst	$r_B \times 10^4$[a] (mol *n*-b/hm^2)	$r_{MA} \times 10^4$[b] (mol MA/hm^2)
VPO	7	5.6
VPOMo1	20	14.4
VPOMo3	10	7.2
VPOMo5	9	3.3

[a] *n*-Butane reaction rate.
[b] Maleic anhydride formation rate.
[c] Reaction conditions: $T = 320°C$; 0.8% *n*-butane in air; $P = 1$ atm.

The higher yield to maleic anhydride obtained in MoVPO compared to unpromoted oxides was obtained when Mo was incorporated by impregnation through increases in both conversion and selectivity. This is in agreement with the results reported by Ye *et al.* (6). When Mo was added by coprecipitation, a decrease in the yield to maleic anhydride was observed as in Takita's catalysts (7). But contrary to what these authors found in our catalyst VPOMo1(co) the decrease in yield is due to a dramatic fall of selectivity despite the fact that the activity is higher than in VPO (Figs. 1A and 1B). However, these results are at variance with the conclusions reached by Hutchings and Higgins (12), who found that when Mo-promoted catalysts were prepared by addition of MoO_3 together with V_2O_5 with a Mo/V ratio of 0.04 at the start of precursor synthesis, catalysts showed higher specific activity and selectivity than the VPO solid without Mo. This confirms that the promoting effect of Mo on VPO solids is also a function of the way the ion was added during the preparation of the $VOHPO_4 \cdot 0.5H_2O$ phase (precursor) and of how this was conducted (12).

The addition of promoters could induce structural as well as electronic changes in the bulk and surface of the catalysts and an ensuing modification of catalytic behavior. In order to elucidate which of such changes were responsible for the increased activity and selectivity of Mo-promoted VPO, several techniques were employed.

No other than $(VO)_2P_2O_7$ phases were detected either by XRD or Raman spectroscopy in the promoted catalysts, which is in agreement with what was reported for comparable systems (6, 8, 12, 13).

Contrary to what was found by other authors, the surface area of the VPO solids remained unaltered after the incorporation of Mo either by impregnation or coprecipitation (6, 7, 12).

From the thickness and R_c (values which characterize the morphology of $(VO)_2P_2O_7$ crystallite), it appears that the Mo added to the $VOHPO_4 \cdot 0.5H_2O$ phase by impregnation did not induce structural changes of the $(VO)_2P_2O_7$ crystallite (Table 3). This suggested that despite the phase transformation that occurs during the activation procedure, which includes the development of an amorphous compound and its transformation into crystallized $(VO)_2P_2O_7$ (11, 23, 24), Mo was not incorporated into the crystal lattice of $(VO)_2P_2O_7$. Further evidence of this was obtained by FTIR; in fact, the band corresponding to V=O did not shift in the promoted VPO solids (Fig. 3A) as was found by Takita *et al.* (7). These authors reported that such band significantly shifted when elements of various electronegativity were incorporated into the lattice by substitution of vanadium by metal.

When Mo was added together with phosphoric acid the thickness of the $(VO)_2P_2O_7$ crystallites shows an erratic behavior. In the 1% Mo solids the plate thickness of the [100] plane was lower than in the VPO oxides. In the 5% Mo solid, it was higher than in the unpromoted samples (Table 3). The surface area and the V=O band shift did not reflect such behavior (Table 3, Fig. 4B) These results seem to suggest that the addition of the promoter is not the sole factor in the morphology changes of the $(VO)_2P_2O_7$ crystallite. The data obtained so far do not allow us to elucidate the reasons for such behavior.

Therefore, it is evident that the promotional effect of Mo would not be exclusively due to structural changes. It could also have an electronic origin which might affect the properties of the $(VO)_2P_2O_7$ phase active sites. In this sense, it was indeed interesting to investigate the acidity property and the oxidation state of vanadium, both in the promoted and in the unpromoted VPO catalysts.

It has been proposed (4) that Lewis sites are associated with surface coordinatively unsaturated (CUS) V^{4+} ions. These sites could be affected by the addition of Mo. The results obtained when the Lewis sites were characterized by acetonitrile adsorption were comparable in VPO, VPOMo1, and VPOMo1(co), after evacuation at room temperatures (Fig. 6A), and they are in agreement with the ones reported by Cornaglia *et al.* (17). After evacuation at 150°C significant differences appear in the VPOMo1 and VPOMo1(co) spectra (Fig. 6B). In the former one, the band assigned to very strong Lewis sites remains intact whereas in the latter such band was totally desorbed. This behavior resembles the one reported by Cornaglia *et al.* (17) when they compared equilibrated and nonequilibrated organic catalysts with aqueous catalysts. In fact they found that only the equilibrated solids retain the very strong Lewis band at temperatures up to 150°C.

It is then clearly suggested that the effect of Mo on the CUS V^{IV}, if any, is a function strongly dependent on how Mo was added to the VPO oxides.

The presence of very strong Lewis sites in VPOMo1 correlates with the higher maleic anhydride yield of this catalyst (Fig. 2B). As was pointed out before this is mainly due to the higher selectivity of such solids compared with VPO1(co) and VPO catalysts (Fig. 1B). This correlation of very strong Lewis sites and selectivity is in line with what was proposed by other authors (4, 17).

It has been frequently suggested that the presence of residual V^V entities on the V^{IV} matrix plays an important role in the *n*-butane transformation to maleic anhydride. However, there is no general consensus related to the nature of such species in the VPO oxides and to the optimal V^V/V^{IV} ratio associated to the best catalytic performance (1, 5, 11, 12, 14). Within this context, it is important to analyze the effect of Mo on the oxidation state of vanadium.

The broadening to the low frequency zone observed in the promoted and unpromoted VPO catalysts when the V=O stretching bands of such solids were compared with the pure $(VO)_2P_2O_7$ phase (Figs. 4 and 5A) could be a consequence of the presence of ν_s P–O bands, characteristic of the α and β phases (Fig. 5A). The results shown in Fig. 5B would give further support to this hypothesis which suggests that after 400 h under reaction stream, the VPO solids some may present some traces of V^V. However, such species appear not to be strongly affected by the addition of Mo, either by impregnation or by coprecipitation (Figs. 4A and 4B).

Results obtained with the more sensitive LRS technique (15, 25) do not allow us to confirm the above hypothesis. Again, the main signals detected in all catalysts are the ones corresponding to $(VO)_2P_2O_7$ phase (Figs. 7 and 8). None of the bands reported for V^V (15, 25), either below 700 cm^{-1} or between 850 and 1200 cm^{-1}, were detected.

In the same vein, XPS results reveal that V^V are not present on the surface of the promoted and unpromoted catalysts after 400 h under reaction stream (Table 4).

In fact, the V2$p_{3/2}$ BE of VPO catalysts and promoted VPO catalysts shows a constant value of 517.9 ± 0.1 eV (Table 4) which could be assigned to the BE of the pure $(VO)_2P_2O_7$ phase of V^{IV}. Besides, when applying peak synthesis, only one component was detected. In any case the statistical parameter of simulation was improved when two components were considered.

At this point it is important to notice that a discrepancy appears in the literature with the BE that corresponds to V^{IV} and V^V depending on the references taken (viz. O1*s* or C1*s*). Values between 517.2 and 517.7 eV for the former and between 518.1 and 518.9 for the latter have been reported by several authors (5, 11, 14, 26). However, the use of the O1*s* reference for the BE would not be the most usual one.

Further evidence of the V^{IV} existence was obtained from the ΔO1*s*-V2$p_{3/2}$ values. A constant value of 14.3 eV was observed in all the catalysts studied against a value of 12.9 eV for V^V in the β-$VOPO_4$ phase (Table 5).

Volta and co-workers (8) in their study over VPO doped with 5% (w/w) of Co^{II} and Fe^{III} found that depending on its redox potential and on its dispersion the promoter controls the V^V/V^{IV} balance during the activation period. Co with a redox potential Co^{III}/Co^{II} (1.85 V/NHE) higher than the redox potential of V^V/V^{IV} (1 V/NHE) increases the V^V/V^{IV} ratio compared with the VPO catalyst, whereas the Fe with a lower potential Fe^{III}/Fe^{II} (0.75 V/NHE) decreases the V^V/V^{IV} ratio.

The Mo introduced as Mo^{VI} in the $VOPO_4 \cdot 0.5H_2O$ precursor (both in the impregnation and in the coprecipitation) is unable to displace V^{IV} to V^V due to its lower redox potential Mo^{VI}/Mo^{IV} (0.645 V/NHE). In addition, the unpromoted VPO catalysts present neither V^V phases nor V^{VI} on the surface (Figs. 7 and 8 and Table 4). Consequently, it is not possible to detect the effect of Mo in lowering the V^V/V^{IV} ratio.

The absence of a detectable amount of V^V in the catalyst under study suggested that promoted and unpromoted catalysts after 400 h under reaction condition show the same valence state of vanadium as the equilibrated catalyst (11). Nevertheless, the yield to maleic anhydride of these catalysts was significantly lower than the equilibrated ones (Fig. 3), and also the solids showed a partially crystallized $(VO)_2P_2O$ phase (Table 3). This confirms what was reported by other authors (11, 23, 24), i.e., that during aging, besides completing the reduction of V^V, the crystallization of vanadyl pyrophosphate occurs. This study suggests, however, that crystallization takes longer than complete reduction. Both transformations play an important role in the development of a catalyst with high yield to maleic anhydride (equilibrated catalyst). Noticeably, whereas XRD showed a comparable crystallinity of all the catalysts (Table 3), the LRS results show a better local order of the promoted catalyst than VPO (Figs. 7 and 8).

Despite the fact that it was not possible to conclude that the addition of Mo to VPO affects the V^{IV}/V^V ratio of such solids, TPR results suggested that more labile oxygens are present in the Mo-impregnated VPO solids compared with both the coprecipitated MoVPO and the unpromoted catalysts (Table 7, Fig. 9). This lability of the oxygen would modify the redox capacity of the VPO oxides and would consequently affect the redox mechanism of the surface layer which is very probably responsible for the selective formation of maleic anhydride from butane (4, 5). Noticeably, the solid with highest reducibility also presented the highest selectivity (Table 7, Figs. 9 and 1B).

Searching for additional evidence of the interaction of the cation with the $(VO)_2P_2O_7$ phase, a comparison of the Raman signals of the P–O–P binding (vide supra) of the promoted and unpromoted catalysts seems appropriate. The incorporation of Mo produces a broadening of the basis of the $(VO)_2P_2O_7$ signal toward higher wavenumbers (Figs. 7 and 8). This could be associated with an increase of the binding angle of P–O–P and an ensuing greater distortion of the O_3P–O–PO_3 structure which, in its turn, could be due to some interaction of the Mo species, occluded between the layers of the $(VO)_2P_2O_7$ phase. No possible effects of Mo on the V–O–P species could be analyzed because such bands (400–600 cm^{-1} region) were detected neither in the VPO nor in the VPOMo samples (Fig. 8). At

this point, it seems relevant to know the nature of such Mo species. As pointed out before, XRD patterns did not detect any crystalline phases of Mo with crystallite size higher than 40 Å. The TPR profiles of the supported MoVPO catalysts did not present a pattern, which could reveal the existence of supported MoO_3 (Fig. 9). In fact, the starting reduction temperature of VPOMo1 was about 500°C, against 400°C for the mechanical mixture of MoO_3 and VPO catalysts. Following the same trend, Cáceres *et al.* (27) and Marchi *et al.* (28) reported starting reduction temperatures of 380 and 350°C for MoO_3 supported on Al_2O_3 and SiO_2, respectively.

In catalysts where Mo was added by coprecipitation, the shape of the TPR profiles did not permit a definitive assertion about the absence of supported MoO_3 (Fig. 9). However, LRS results strongly suggested that MoO_3 are not present in either impregnated or coprecipitated MoVPO catalysts. In fact, no isolated signal characteristic of such oxides appeared in any of the solids studied (Figs. 7 and 8). Despite the difficulty in identifying the symmetric stretching band of mono-oxo terminal bindings of MoO_3 in the 1000 cm^{-1} region due to the existence of the same type of signal of the V=O of the $(VO)_2P_2O_7$ phase, it was clear that no signal corresponding to Mo–O–Mo binding appeared in the 800–600 cm^{-1} region (Figs. 7 and 8).

This seems to confirm the absence of polymeric MoO_3 species. If there were any, they would be highly dispersed and with a monomeric structure.

One of the most remarkable features of molybdenum is its chemical versatility (29). Consequently, different species could be formed depending on the preparation of MoVPO solids. When Mo as ammonium heptamolybdate was added together with the phosphoric acid (vide supra), the molybdate ions appeared in an organic solution containing other oxions such as PO_4^{3-} and VO^{2+}. The pH of the solution ($pH < 4$) could facilitate the formation of heteropolyanion (29, 30) (viz. $PMo_{11}VO_{40}^{-4}$). Nevertheless, with the results obtained so far, it was not possible to detect such kinds of species (Figs. 7 and 8). XPS results of coprecipitated MoVPO catalysts only show the presence of Mo^{VI} (Table 5) which rules out any reduction of the ion both in the preparation step and under reaction conditions.

When Mo was added by impregnation of $(VO)HPO_4 \cdot 0.5H_2O$, a solid solution formation of a mixed V and Mo phase could occur (12, 31). The supported MoVPO's presented both Mo^{VI} and Mo^{IV} on the surface (Table 5). This suggests that the $MoOPO_4$ phase proposed by Hutchings and Higgins (12) is not present on the surface of $(VO)_2P_2O_7$. Reduction of Mo^{VI} to Mo^{IV} would occur during the precursor activation. Noticeably, the catalyst with higher yield to maleic anhydride (viz. VPOMo1) also presented the highest Mo^{IV}/Mo^{VI} ratio of all the impregnated Mo catalysts (Fig. 2B and Table 7).

Another important piece of information obtained from the analysis of XPS data is the catalyst surface molybdenum enrichment observed in both the impregnated and the coprecipitated MoVPO solids (Tables 1 and 5). This enrichment seems not to correlate with the activity and selectivity of the catalyst (Fig. 1A and 1B, Table 7).

Finally, it should be pointed out that molybdenum-based catalysts are widely used in oxidation reactions (31). Consequently, a direct contribution of Mo species in modifying the selectivity of the *n*-butane partial oxidation to maleic anhydride could not be ruled out with the results obtained so far. Further studies are necessary to elucidate this topic.

CONCLUSIONS

- The addition of Mo by impregnation of the $VOHPO_4 \cdot 0.5H_2O$ increases the yields to maleic anhydride and the specific activity of VPO catalysts (Figs. 1 and 2 and Table 8).
- The promoting effect is a function of both the Mo loading and the way in which such cation was added. When Mo was incorporated during the preparation of the precursor ($VOHPO_4 \cdot 0.5H_2O$ phase). This effect also depended on how this was conducted (Figs. 1 and 2) (12).
- The best catalyst was obtained when Mo was added by impregnation with 1% Mo ($Mo/V = 0.02$, Figs. 1–3).
- The structure of $(VO)_2P_2O_7$, as well as the BET surface area, the exposure of the [100] plane, and the disorder along [100] planes, seems not to depend too strongly on the addition of Mo by impregnation of the $VOHPO_4 \cdot 0.5H_2O$ phase (Table 3). No incorporation of the promoter element into the crystal lattice was detected (Figs. 4 and 5). Only a local distortion of the O_3–P–O–PO_3 structure (increase of the P–O–P binding angle) was observed. (Figs. 7 and 8).
- The promotional effect of Mo would be electronic in origin (12) in which the very strong Lewis acid sites and the lability of the structure oxygen were enhanced (Figs. 6 and 9 and Table 7).
- Polymeric MoO_3 species are not present in either impregnated or coprecipitated MoVPO catalysts (Figs. 7–9). In the latter ones, only Mo^{VI} entities would exist on the surface layer, whereas in the former one, Mo^{VI} and Mo^{IV} species coexist. The nature of such species is not known at this time, but the catalyst with the highest yield to maleic anhydride has the highest Mo^{IV}/Mo^{VI} surface ratio (Table 5).
- In agreement with other authors (11, 23, 24) this study confirms the role ascribed to the activation procedure which involves the transformation of $VOHPO_4 \cdot 0.5H_2O$, the complete reduction of V^V to V^{IV}, and the crystallization of the $(VO)_2P_2O_7$. Each transformation needs different times during the aging procedure to obtain the equilibrated catalyst. Promoters may also play a role in such a procedure (Fig. 7).

REFERENCES

1. Centi, G., *Catal. Today* **16**, 5 (1993).
2. Hutchings, G., *Appl. Catal.* **72**, 1 (1991).
3. Hutchings, G., Demantin Chanel, A., Olier, R., and Volta, J. C., *Nature* **368**, 41 (1994).
4. Abon, M., and Volta, J. C., *Appl. Catal. A: General* **157**, 173 (1997).
5. Koyan, G., Okuhara, T., and Misono, M., *J. Am. Chem. Soc.* **120**, 767 (1998).
6. Ye, D., Satsuma, A., Hattori, A., Hattori, T., and Murakami, Y., *Catal. Today* **16**, 113 (1993).
7. Takita, Y., Tanaka, K., Ichinaru, S., Mizihara, Y., Abe, Y., and Ishihara, T., *Appl. Catal. A: General* **103**, 281 (1993).
8. Ben Abdelouahab, F., Olier, R., Ziged, M., and Volta, J. C., *J. Catal.* **157**, 687 (1995).
9. Sananés Schultz, M. T., Ben Abdelouahad, F., Hutchings, G., and Volta, J. C., *J. Catal.* **163**, 346 (1996).
10. Koyan, G., Okuhara, T., and Misono, M., *Catal. Lett.* **32**, 200 (1995).
11. Albonetti, S., Cavani, F., Trifirò, F., Venturoli, P., Calestani, G., Granados, M. L., and García Fierro, J. L., *J. Catal.* **160**, 52 (1996).
12. Hutchings, G., and Higgins, R., *J. Catal.* **162**, 153 (1996).
13. Bej, S. K., and Rao, M. S., *Appl. Catal. A: General* **83**, 149 (1992).
14. Cornaglia, L., and Lombardo, E., *Appl. Catal. A: General* **127**, 125 (1995).
15. Ben Abdelouahab, F., Olier, R., Lefebvre, G., and Volta, J. C., *J. Catal.* **134**, 151 (1992).
16. Bordes, E., and Contractor, R., *in* "Preparation of Catalysts VI" (G. Poncelet *et al.*, Eds.), *Stud. Surf. Sci. Catal.* **91**, 707 (1995).
17. Cornaglia, L., Lombardo, E., Anderson, J. A., and García Fierro, J. L., *Appl. Catal. A: General* **100**, 37 (1993).
18. Busca, G., Centi, G., Trifirò, F., and Lorenzelli, V., *J. Phys. Chem.* **90**, 1337 (1986).
19. Cornaglia, L., Caspani, C., and Lombardo, E., *Appl. Catal.* **74**, 15 (1991).
20. Nakamoto, K, "Infrared and Raman Spectra of Inorganic and Coordination Compounds," 4th ed., p. 168. Wiley, New York, 1986.
21. Vuurman, M., and Wachs, I., *J. Phys. Chem.* **96**, 5008 (1992).
22. Wachs, I. E., *Catal. Today* **27**, 437 (1996).
23. Sola, G. A., Pierini, B. T., and Petunchi, J. O., *Catal. Today* **15**, 537 (1992).
24. Zhang-Lin, Y., Forissier, M., Védrini, J. C., and Volta, J. C., *J. Catal.* **145**, 226 (1993).
25. Guliants, V. V., Benziger, J. B., Sundaresan, S., Wachs, I. E., Jehng, J. M., and Roberts, J. E., *Catal. Today* **28**, 275 (1996).
26. López Granados, M., Coronado, J. M., García Fierro, J. L., Cavani, F., Giuntoli, F., and Trifirò, F., *Surf. Inter. Anal.* **25**, 667 (1997).
27. Cáceres, C. V., García Fierro, J. L., López Agudo, A., Blanco, M. N., and Thomas, H. J., *J. Catal.* **95**, 501 (1985).
28. Marchi, A. J., Lede, E. J., Requejo, F. G., Rentería, M., Irusta, S., Lombardo, E. A., and Miró, E. E., *Catal. Lett.* **48**, 47 (1997).
29. Rollinson, C. L., "The Chemistry of Chromium, Molybdenum and Tugnsten," p. 700. Pergamon, Elmsford, NY, 1993.
30. Misono, M., *Catal. Rev. Sci. Eng.* **29**(2–3), 269 (1987).
31. Trifirò, F., *Catal. Today* **41**, 21 (1998).